Supplementary Material: Panoramic Stereo Videos with a Single Camera

Rajat Aggarwal* Amrisha Vohra* Anoop M. Namboodiri
Kohli Center on Intelligent Systems,
International Institute of Information Technology- Hyderabad, India.
{rajat.aggarwal@research, amrisha.vohra@research, anoop@}.iiit.ac.in

1. Introduction

This supplementary document provides additional details as well as experimental results that could not be included in the main paper due to lack of space. Detailed steps of the derivations that were given in the main paper are provided in Section 2 and 3 along with explanation of each step. Section 4 includes additional results of recovered panoramas and stereo depth estimates that were captured using our proposed setup. More results including anaglyph images, videos of dynamic scenes and stereo depth maps may be found at the project website [1]

2. Optimality of the Surface Shape

In this section, we explain the reason for choosing paraboloid surface for the design of coffee-filter mirror. Let us take a general quadric surface equation, $a_1x^2 + a_2y^2 + a_3z^2 + a_4x + a_5y + a_6z + a_7 = 0$. For a flat surface, a_1, a_2, a_3 are zero, for a paraboloid surface a_3, a_4, a_5 are zero and for hyperboloid surfaces a_4, a_5, a_6 are zero. To calculate the variation in the resolution of the image captured along a radial line, we find the difference between the direction of the consecutive incident rays. In the case of orthographic projections, direction of reflected light rays is same and the direction of incident light rays is directly proportional to normals of the mirror's surface. We find the variation of normals n_v which is given by,

$$n_v = \begin{bmatrix} \cos\theta & \sin\theta & \frac{dz}{dr} \end{bmatrix} \tag{1}$$

for a constant θ and varying r. We find $\frac{dn_v}{dr}$ by,

$$\frac{dn_v}{dr} = \begin{bmatrix} 0 & 0 & \frac{d^2z}{dr^2} \end{bmatrix}$$

Using $x = r\cos\theta$ and $y = r\sin\theta$, we get a general quadratic function given by $f(r, z, \theta)$.

$$f(r,z,\theta) = a_1r^2\cos^2\theta + a_2r^2\sin^2\theta + a_3z^2 + a_4r\cos\theta + a_5r\sin\theta + a_6z + a_7$$

Double differentiating $f(r, z, \theta) = 0$, we get,

$$\frac{d^2f}{dr^2} = 2a_1\cos^2\theta + 2a_2\sin^2\theta + 2a_3\frac{dz}{dr}^2 + 2a_3z\frac{d^2z}{dr^2} + a_6\frac{d^2z}{dr^2}$$

Consider the case of a flat mirror, where $a_1 = 0, a_2 = 0, a_3 = 0$, we get $\frac{d^2z}{dr^2} = 0$, which means that the flat surface has uniform field of view and does not change with r. This means that the field of view is totally dependent upon the height of the mirror.

For the case of a paraboloidal surface, where $a_3 = 0$, we get,

$$\frac{d^2z}{dr^2} = \frac{-2(a_1\cos^2\theta + a_2\sin^2\theta)}{a_6} \tag{2}$$

which means that the resolution for the paraboloidal surface is uniformly increasing with respect to r. As r increases, resolution increases. Also the FOV captured in paraboloidal shape is more than that of the flat mirror.

Considering hyperboloidal surface, where $a_6 = 0$, we get,

$$\frac{d^2z}{dr^2} = \frac{-2(a_1\cos^2\theta + a_2\sin^2\theta + a_3\frac{dz^2}{dr})}{a_6 + 2a_3z} \tag{3}$$

Although, FOV is more than that captured by the flat mirror, the resolution increases non-uniformly with r. The resolution difference between the pixels at the upper part of the design and the lower part of the design is drastically high, which makes the choice of hyperbolic design irrelevant.

*Equal Contribution
[1] http://cvit.iiit.ac.in/research/projects/panoStereo/

3. Mirror Surface Derivations

In this section we derive the equation of the mirror surface. Multiple factors can be varied to make the device adaptive to specific applications. We derive the expressions for only one petal APB as shown in the Fig. 1a. and the same expressions hold for all n petals rotated by $2\pi/n$. Circular surfaces AP and PB are used to capture the right and left eye view respectively. Let us consider the angle between the chords of these two faces as β such that $\angle APB$ = β. Each petal subtends an angle θ at the center, where $\theta = \frac{2\pi}{n}$ such that $\angle AOB = \theta$. Hence, we get n views each for left and right eye. The design of the mirror is symmetrical, and all the petals are of same size and dimensions. The length of each face, referred as *petal length*, denoted by l, as shown in Fig. 1a. Each petal, say P_i , where $i = 1$ to n is bounded by a circle C_{max} with radius R_{max}, and inside by a circle C_{min} with radius R_{min}. V is the viewing circle with radius equal to b. From Fig. 1a, $OA = R_{min}$ and $OP = R_{max}$. From $\triangle OAP$ and $\triangle OBP$, by sine rule we get the relations as,

$$\frac{l}{\sin(\frac{\theta}{2})} = \frac{R_{max}}{\sin(\pi - \frac{(\theta+\beta)}{2})} = \frac{R_{min}}{\sin(\frac{\beta}{2})} \tag{4}$$

Since each face is symmetrical and oriented at equal separation,. OP is the angle bisector of the $\angle APB$, such that

$$\angle APO = \angle BPO = \frac{\beta}{2}$$
$$\angle AOP = \angle POB = \frac{\theta}{2}$$

Therefore, in $\triangle OAP$ we get

$$\angle OAP = \pi - \angle APO - \angle AOP$$
$$\angle OAP = \pi - \frac{\theta}{2} - \frac{\beta}{2}$$

Since, LD is the perpendicular bisector of the chord AP and is tangent to the viewing circle V, $\angle DLP$ and $\angle CDO$ are the right angles and $LP = l/2$. $OD = b$ is the radius of the viewing circle. In $\triangle OCD$ and $\triangle CLP$, we get

$$LP = CP\cos(\frac{\beta}{2})$$
$$CP = LP\sec(\frac{\beta}{2})$$
$$= \frac{l}{2}\sec(\frac{\beta}{2}).$$

We know, $OC + CP = R_{max}$, which gives

$$OC = R_{max} - \frac{l}{2}\sec(\frac{\beta}{2}) \tag{5}$$

In $\triangle PLC$,

$$\angle LCP = \pi - \angle CLP - \angle CPL$$
$$= \frac{\pi}{2} - \frac{\beta}{2}$$

$\angle OCD = \angle LCP$ being vertically opposite angles. Thus we get,

$$\angle COD = \frac{\pi}{2} - \angle OCD$$
$$= \frac{\pi}{2} - (\frac{\pi}{2} - \frac{\beta}{2})$$
$$= \frac{\beta}{2}$$

In $\triangle OCD$,

$$\frac{OD}{OC} = \cos\frac{\beta}{2}$$

$$OC = b\sec(\frac{\beta}{2}) \tag{6}$$

Comparing Eqn 5 and Eqn 6 we get

$$R_{max} - \frac{l}{2}\sec(\frac{\beta}{2}) = b\sec(\frac{\beta}{2})$$

$$R_{max} = (b + \frac{l}{2})\sec(\frac{\beta}{2}). \tag{7}$$

Combining Eqn 4 and Eqn 7, we get:

$$2R_{max}\cos\frac{\beta}{2} = 2b + l$$
$$2R_{max}\cos\frac{\beta}{2} = 2b + R_{max}\frac{\sin\frac{\theta}{2}}{\sin\frac{\theta+\beta}{2}}$$

$$R_{max}\left(\frac{(2\cos\frac{\beta}{2}\sin\frac{\theta+\beta}{2}) - \sin\frac{\theta}{2}}{\sin\frac{\theta+\beta}{2}}\right) = 2b$$
$$R_{max}\left(\frac{(2\cos\frac{\beta}{2}(\sin\frac{\theta}{2}\cos\frac{\beta}{2} + \cos\frac{\theta}{2}\sin\frac{\beta}{2})) - \sin\frac{\theta}{2}}{\sin\frac{\theta+\beta}{2}}\right) = 2b$$
$$R_{max}\left(\frac{(2\cos^2\frac{\beta}{2} - 1)\sin\frac{\theta}{2} + \cos\frac{\theta}{2}(2\sin\frac{\beta}{2}\cos\frac{\beta}{2})}{\sin\frac{\theta+\beta}{2}}\right) = 2b$$
$$R_{max}\left(\frac{\cos\beta\sin\frac{\theta}{2} + \cos\frac{\theta}{2}\sin\beta}{\sin\frac{\theta+\beta}{2}}\right) = 2b$$

$$R_{max}\left(\frac{\sin\frac{\theta+2\beta}{2}}{\sin\frac{\theta+\beta}{2}}\right) = 2b \tag{8}$$

Combining Eqn 4 and Eqn 8, we get

$$R_{max} = \frac{2b\sin(\frac{\theta+\beta}{2})}{\sin(\frac{\theta+2\beta}{2})} \tag{9}$$

$$R_{min} = R_{max}\frac{\sin(\frac{\beta}{2})}{\sin(\frac{\theta+\beta}{2})} = \frac{2b\sin(\frac{\beta}{2})}{\sin(\frac{\theta+2\beta}{2})} \tag{10}$$

$$l = R_{max}\frac{\sin(\frac{\theta}{2})}{\sin(\frac{\theta+\beta}{2})} = \frac{2b\sin(\frac{\theta}{2})}{\sin(\frac{\theta+2\beta}{2})} \tag{11}$$

3.1. Selection of optimal parameters

In our proposed design, disparity and device size can be altered depending upon the application requirement. Size of the device is proportional to R_{max}. In order to have a compact design of the mirror that generates human perceivable stereo panoramas, the design parameters need to be optimized.

3.1.1 Optimal outer radius

The value of the outer radius of the coffee filter mirror i.e. R_{max} is dependent upon β. We minimize the parameter R_{max} as given by Eqn 9 and get an optimal petal angle,

$$\boxed{\beta_{opt} = \frac{\pi-\theta}{2}} \tag{12}$$

at which R_{max} is minimum, and hence we get the minimum size of the device.

3.1.2 Optimal angle between the two petals

We now find the optimal angle between the two petals. In Fig. 1a, Let $\angle PBE$ be α, the angle between two petals.

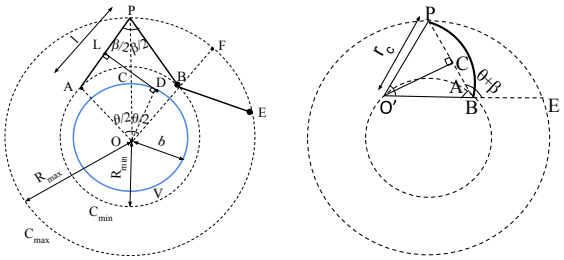

Figure 1: Geometry of the petal surface used to obtain optimal design parameters.

Consider $\triangle OBP$ where

$$\angle OPB = \frac{\beta}{2}, \angle POB = \frac{\theta}{2}$$
$$\angle OBP = \pi - \frac{\theta+\beta}{2}$$

Therefore

$$\begin{aligned}\angle PBF &= \pi - \angle OBP \\ &= (\pi - \frac{\theta+\beta}{2}) \\ &= \frac{\theta+\beta}{2}\end{aligned}$$

Since OP is the angle bisector at equal separation, $\angle PBE = 2\angle PBF$, which means $\alpha = \theta+\beta$, which means $\alpha_{opt} = \theta + \beta_{opt}$. Hence, from Eqn 12 we get

$$\boxed{\alpha_{opt} = \theta + \frac{\pi-\theta}{2} = \frac{\pi+\theta}{2}} \tag{13}$$

3.1.3 Optimal angular curvature of a face

Next, we find the optimal value of the angular curvature of a face. Consider Fig. 1b where O' is the center of curvature of the face PB. PO' and $O'B$ are the radii of curvature i.e r_c and $\angle PO'B = 2\gamma$ is the angle subtended by each face at the center of curvature. In $\triangle PO'B$, $\angle A = \pi - (\theta+\beta)$, which implies,

$$\gamma = \frac{\pi}{2} - \angle A = (\theta+\beta) - \frac{\pi}{2}$$

In order to have a smaller device size,

$$\gamma_{opt} = (\theta + \beta_{opt}) - \frac{\pi}{2}$$

Therefore, the optimal horizontal angular field of view is given by:

$$\boxed{\gamma_{opt} = \frac{\theta}{2}} \tag{14}$$

and is independent of the obtuse angle $\angle PBE$ between two adjacent petals.

3.1.4 Optimal Radius of the curvature

From Fig 1b, $O'C$ is the perpendicular bisector of PB, $CB = \frac{l}{2}$. In $\triangle O'CB$, $\frac{l/2}{r_c} = \sin\gamma$. Radius of curvature r_c can be optimized by using the optimal value of γ. Therefore,

$$\boxed{r_{c_{opt}} = \frac{l}{2\sin\frac{\theta}{2}}} \tag{15}$$

is the optimal radius of curvature. It is to be noted that these centers of curvature lie on a circle.

To avoid wastage of pixels due to inter-reflections, as explained in Section 4.2 in the main paper, it is important to collect the maximum scene information in the captured image. Each face covers $\frac{2\theta}{n}$ angular FOV, thus a total of n such faces for each view covers complete 2π FOV. For no missing regions, FOVs of two faces for the same eye views should be covering consecutive areas of the scene. This is achieved by aligning one face in the direction of $O'P$ and the next face for the same eye view, in the direction BE. Hence the obtuse angle between the two faces PB and BE is $\frac{\pi+\theta}{2}$. The amount of inter-reflections depends upon the angle between two consecutive petals, α, which depends upon the sampling angle of the device $\frac{2\pi}{n}$. Ideally, the amount of inter-reflections reduces down to zero, when the FOV of two consecutive faces do not intersect at all. However, this way, some of the scene regions will be left uncovered in the FOV of some faces and hence not imaged at all. In order to account for these inter-reflections, we introduce a small angle δ such that the angle of curvature becomes $2\gamma+\delta$. This makes sure some overlap is there, so that some redundant information is captured, which can be used while dewarping. However, the value of δ is kept sufficiently low, such that inter-reflections are also reduced to a huge extent.

3.2. Resultant Mirror Surface

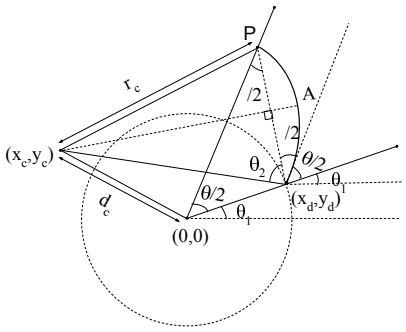

Figure 2: Parameters of the mirror petal.

In this section, we obtain the surface equations of the proposed coffee filter mirror in terms of polar coordinates ϕ and r. As explained earlier, the surface of the *coffee filter mirror* is paraboloidal vertically and circular in each horizontal cross section. Let us consider the central axis of the mirror to be the z axis. Then the surface equation can be written as a function of x and y axis:

$$z = f(x, y) = m_\phi(x^2 + y^2), \tag{16}$$

where m_ϕ is the slope of the parabola for a given ϕ. Let $x^2+y^2 = r^2$, where r is the radial distance in the XY plane and ϕ is the angle of the radial line, then:

$$z = m_\phi r^2 \tag{17}$$

Eqn 17 represents the petal surface of our custom designed mirror centered around origin. Consider the uppermost and widest cross section of the mirror at $z = z_{max}$, such that

$$z_{max} = m_\phi {r_1}^2$$
$$m_\phi = \frac{z_{max}}{r_1^2}$$

Let (x_c, y_c) be the center of the circle of curvature of a face of a petal and (x_d, y_d) be the point which lie on the curvature, $r_1^2 = k^2 r^2$ such that $x_d = kx$ and $y_d = ky$. r_c be the radius of the circle of curvature for a face. Combining this with Eqn 17, we get

$$m_\phi = \frac{z_{max}}{k^2 r^2}$$

which implies

$$z = \frac{z_{max}}{k^2}$$

Distance between $(0, 0)$ and (x_c, y_c) is d_c such that $x_c^2 + y_c^2 = d_c^2$, Calculating distance from center of the curvature and the point on the curvature we have:

$$(x_d - x_c)^2 + (y_d - y_c)^2 = r_c^2$$
$$(kx - x_c)^2 + (ky - y_c)^2 = r_c^2$$

$$\implies k = \frac{(xx_c + yy_c) + \sqrt{(xx_c + yy_c)^2 - r^2(d_c^2 - r_c^2)}}{r^2}$$

Since, $m_\phi = z_{max}/k^2 r^2$,

$$m_\phi = z_{max}\left(\frac{r}{(xx_c + yy_c) + \sqrt{(xx_c + yy_c)^2 - r^2(d_c^2 - r_c^2)}}\right)^2$$

Also, from the Fig. 2, it is to be noted that (x_c, y_c) forms angle $\theta_1 + \frac{\theta}{2} + \frac{\beta}{2} + \theta_2$ from the horizontal. Hence,

$$x_c = x_d + r_c(\cos(\theta_1 + \frac{\theta}{2} + \frac{\beta}{2} + \theta_2)$$
$$y_c = y_d + r_c(\sin(\theta_1 + \frac{\theta}{2} + \frac{\beta}{2} + \theta_2))$$

where $\theta_2 = \tan^{-1}(\frac{2r_c}{l})$.
From this and Eqn 17 we get,

$$z = z_{max}\left(\frac{r^2}{(xx_c + yy_c) + \sqrt{(xx_c + yy_c)^2 - r^2(d_c^2 - r_c^2)}}\right)^2 \tag{18}$$

Therefore, Eqn 18 gives the equation of the paraboloidal surface of the mirror. Note that the slope m_ϕ at every point is a function of r.

3.3. Estimation of Surface normals

In this section, we derive the equation of the normal vector of a point on coffee-filter mirror. Let $\hat{\mathbf{n}}$ be the direction of the normal vector of point $P(r, \phi)$. We find $\hat{\mathbf{n}}$ by finding the normal vector of the tangent plane at point $P(r, \phi)$ which consists of tangent vectors in horizontal and vertical plane such that $\hat{\mathbf{n}} = \mathbf{PA} \times \mathbf{PB}$. $\mathbf{PA}$ and $\mathbf{PB}$ are the tangent vectors at point P in the horizontal and vertical direction respectively.

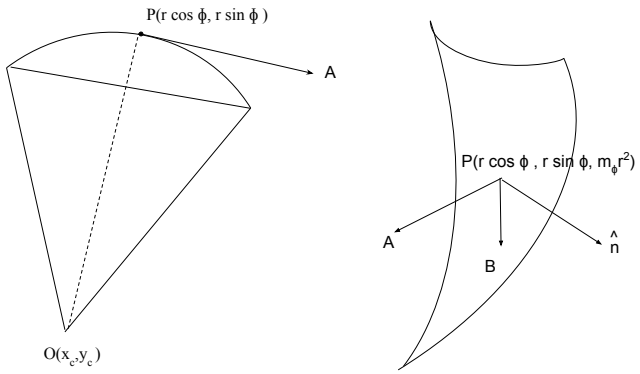

Figure 3: Geometry for deriving the normals direction at point $\mathbf{P}$.

Let us consider the horizontal plane containing point P as shown in Fig. 3a where P lies on a circular curvature with center O such that $P = (r\cos\phi, r\sin\phi, z_0)$, $O = (x_c, y_c, z_0)$ and

$$\mathbf{OP} = \mathbf{P} - \mathbf{O} = \begin{bmatrix} r\cos\phi - x_c & r\sin\phi - y_c & 0 \end{bmatrix}^T$$

And the vector PA which is orthogonal to OP is this given by:

$$\mathbf{PA} = \mathbf{n_h} = \begin{bmatrix} y_c - r\sin\phi & r\cos\phi - x_c & 0 \end{bmatrix}^T$$

Similarly we calculate $\mathbf{PB}$ in the vertical direction for a fixed ϕ, where $P(x, y, z) = (r\cos\phi, r\sin\phi, m_\phi r^2)$ such that $\mathbf{PB}$ is given by

$$\begin{aligned} \mathbf{PB} = \mathbf{n_v} &= \begin{bmatrix} \frac{dx}{dr} & \frac{dy}{dr} & \frac{dz}{dr} \end{bmatrix}^T \\ &= \begin{bmatrix} \cos\phi & \sin\phi & 2m_\phi r \end{bmatrix}^T \end{aligned}$$

In the end, we calculate $\mathbf{n}$ as $\mathbf{n} = \hat{\mathbf{PA}} \times \hat{\mathbf{PB}} = \hat{\mathbf{n_h}} \times \hat{\mathbf{n_v}}$.

3.4. Epipolar Geometry and Stereo Depth Estimation

In this section we explain the derivation of the epipolar geometry in detail. In general, epipolar geometry is used for reducing the search space of matching points in the two stereo images. In our device setup, the arrangement of the mirrors capturing both left and right eye views, enables us to calculate the epipolar geometry by finding the direction of incident rays which are captured using the parabolic reflector. As described in the Section 5.3 in the main paper, the conventional camera used in the system captures the light rays which are parallel to the central axis of the camera using a parabolic reflector. Hence, all the rays which are incident on the coffee-filter mirror are reflected in the parallel direction. From the surface normals derived in the previous section, we find out the direction of the set of the incident rays captured using the proposed system.

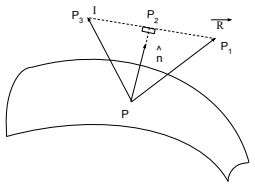

Figure 4: Geomtery for deriving the direction of incident ray direction.

Consider Fig. 4 where $\mathbf{I}$ is the Incident ray vector on any point, $\mathbf{n}$ is the normal vector and $\mathbf{R}$ is the reflected ray vector. Since the direction of reflected ray and the normal vector is already known, we calculate the direction of the incident ray to calculate the epipolar lines. From $\triangle PP_2P_3$, $\mathbf{P_2P_3}$ is the projection of $\mathbf{PP_3}$ on $\mathbf{PP_2}$. Hence,

$$\begin{aligned} \mathbf{P_3P_2} &= \mathbf{PP_2} - \hat{\mathbf{I}} \\ &= (\mathbf{PP_3} \cdot \hat{\mathbf{PP_2}})\hat{\mathbf{PP_2}} - \hat{\mathbf{I}} \\ &= (\mathbf{I} \cdot \hat{\mathbf{n}})\hat{\mathbf{n}} - \hat{\mathbf{I}} \end{aligned}$$

Applying laws of reflection, the triangles $\triangle PP_3P_2$ and $\triangle PP_1P_2$ are congruent. This means,

$$\begin{aligned} \mathbf{P_3P_1} &= 2\mathbf{P_3P_2} \\ &= 2((\mathbf{I} \cdot \hat{\mathbf{n}})\hat{\mathbf{n}} - \hat{\mathbf{I}}). \end{aligned}$$

Applying vector triangle law in $\triangle P_1P_2P_3$ we get,

$$\begin{aligned}\mathbf{PP_1} &= \mathbf{PP_3} + \mathbf{P_3P_1} \\ &= \hat{\mathbf{I}} + 2((\mathbf{I}\cdot\hat{\mathbf{n}})\hat{\mathbf{n}} - \hat{\mathbf{I}}) \\ &= 2(\mathbf{I}\cdot\hat{\mathbf{n}})\hat{\mathbf{n}} - \hat{\mathbf{I}} \\ \hat{\mathbf{R}} &= 2(\mathbf{I}\cdot\hat{\mathbf{n}})\hat{\mathbf{n}} - \hat{\mathbf{I}}\end{aligned}$$

Using principle of reversibility of light, one can simply derive

$$\hat{\mathbf{I}} = 2(\mathbf{R}\cdot\hat{\mathbf{n}})\hat{\mathbf{n}} - \hat{\mathbf{R}}$$

With our setup the $\hat{\mathbf{R}}$ is known, $\hat{\mathbf{I}}$ becomes the function of r, ϕ for each point on the surface.

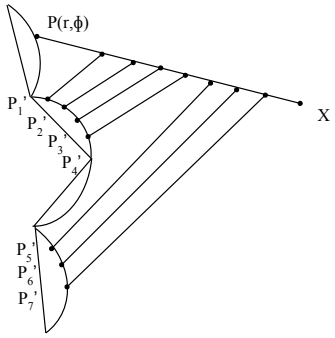

Figure 5: Geometry showing the set of the points viewing the straight line **X** to derive the epipolar constraints.

Let us consider a point in 3D world as shown in Fig. 5 defined by (X, Y, Z) which is imaged by a mirror surface at point $P(r, \phi)$, then the incident ray direction $\hat{\mathbf{I}}$ at P is viewed by some other mirror surface at location $P'(r', \phi')$. The set of such points form an epipolar curve for the point P. Epipolar curve for a point in the left face is found by minimizing the distance between the incident rays from a point in a left face P to every other point in it's right face P'. Thus, for each ϕ in the mirror surface, we find the r_ϕ which intersects the reflected ray from point P such that the triple vector product is zero which means,

$$\frac{|[\mathbf{PP'}, \mathbf{I}_{\mathbf{r},\phi}, \mathbf{I}_{\mathbf{r'},\phi'}]|}{|\mathbf{I}_{\mathbf{r},\phi} \times \mathbf{I}_{\mathbf{r'},\phi'}|} = 0 \tag{19}$$

where $\mathbf{I}_{\mathbf{r},\phi}$ represents the direction of reflected ray from mirror surface.

Each point is then transformed into the corresponding image coordinate using the dewarping method explained in previous section. Since, the design behaves as a non-central camera, every point has different epipolar constraints. We calculate stereo disparity between the left and right views by finding the correspondences along these epipolar curves using sum of squared differences (SSD). For this, we formulate this problem as energy minimization problem and find solution using [1].

3.5. Derivation of Orthographic Projections

We observed that for most practical applications, important information perceived by humans is in the lower part of the world whereas upper part is mostly the sky. In our design, owing to the structure, upper part of the surface has better resolution than the lower regions. Therefore, we keep the coffee filter design inverted as shown in Fig. 6. A parabolic reflector is kept above it, both aligned along the same central axis. This parabolic mirror captures the orthographic rays and reflects them at the camera kept at its focus C.

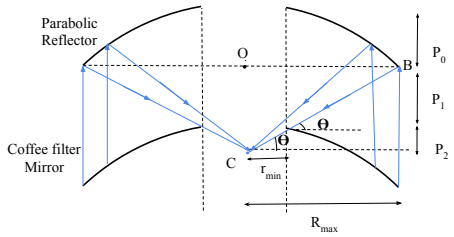

Figure 6: Orthographic Projections using the proposed set up which includes the *coffee filter mirror* and a parabolic reflector

A hole of radius r_{min} is kept in the mirror so that the camera can capture the parallel rays reflected from the parabolic reflector. Also, $OB = R_{max}$ so that it captures all the rays coming from the entire radius of the mirror surface. Let a be the curvature of the parabolic reflector such that the equation of the parabolic reflector can be represented as

$$z = ar^2 \tag{20}$$

then $p_0 = aR_{max}^2$. Also, from Fig. 6:

$$\tan\Theta = \frac{p_1}{R_{max} - r_{min}} = \frac{p_2}{r_{min}} \tag{21}$$

Since, $\frac{1}{4a}$ is the focal length of the parabolic reflector,

$$p_0 + p_1 + p_2 = \frac{1}{4a} \tag{22}$$

Solving Eqns 21 and 22, we get:

$$aR_{max}^2 + p_1 + p_2 = \frac{1}{4a}$$
$$4a^2R_{max}^2 + 4a(p_1 + p_2) - 1 = 0$$
$$(4R_{max}^2)a^2 + 4(p_1 + p_2)a - 1 = 0$$

Solving for a, we get,

$$a = \frac{\sqrt{(p_1 + p_2)^2 + R_{max}^2} - (p_1 + p_2)}{2R_{max}^2} \quad (23)$$

which can be used to find the surface equations of the parabolic reflector.

3.6. Calibration of the Proposed System

In this section, we explain the calibration and dewarping process in detail. As explained earlier that the surface of the mirror is paraboloidal, the resolution is different at different points along each radial line. Also, each captured image depends upon the orientation and viewing angle of the camera. However, for stereo vision to be perceivable, camera's viewing axis must be aligned with the central axis of the device. To calibrate our device, we project structured light binary patterns onto a display surface. These patterns are used to compute a mapping from world coordinates to image coordinates which is used for de-warping the panoramas. We use the approach proposed in [3] and project both normal and inverse binary sequence patterns. These calibration images together will be used to de-warp the captured scene image into left and right eye panoramas as explained in the following steps.

1. **Decoding the calibration images:** At each pixel in the captured image, we find the row and column it corresponds to in the de-warped panoramas, by decoding the observed binary sequence from the calibration images at that particular pixel.

2. **Finding the correct eye views:** For each pixel in the captured scene image we find out the angle of the radial line it lies on from the center of the image. Each petal subtends an angle θ at the center. So pixels at angles 0 to $\frac{\theta}{2}$ belong to the left eye views, and those on angles between $\frac{\theta}{2}$ to θ belong to right eye views.

3. **Creating the left and right panoramas:** The captured scene image is de-warped into left and right panoramas using the spatial information obtained from step 1 and 2. The upper part of the image is of lesser resolution than the lower one. As a result, some portion of de-warped panorama has holes which can be easily filled by interpolating those regions.

4. Additional Results

The dewarped left and right eye panoramas of two scenes are given in Figures 8 and 9 along with red-cyan anaglyph stereo.

Fig 9 below shows the anaglyph of an indoor scene along with the depth values that are recovered from our camera. Even through the design process is optimized for human consumption, the recovered stereo is highly consistent with the ground truth (See Figures 7b and 7c).

References

[1] Y. Boykov, O. Veksler, and R. Zabih. Fast approximate energy minimization via graph cuts. *Pattern Analysis and Machine Intelligence, IEEE Transactions on*, 23:1222–1239, 2001. 6

[2] F. Devernay and S. Pujades. Focus mismatch detection in stereoscopic content. In *IS&T/SPIE Electronic Imaging*. International Society for Optics and Photonics, 2012. 8

[3] J. Posdamer and M. Altschuler. Surface measurement by space-encoded projected beam systems. *Computer graphics and image processing*, 18:1–17, 1982. 7

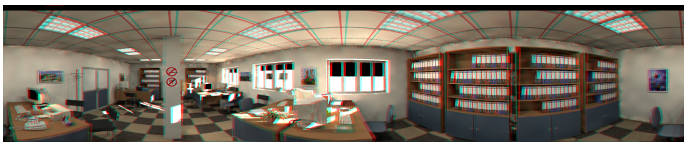

(a)

(b)

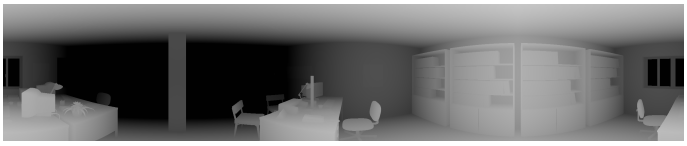

(c)

Figure 7: (a) The red-cyan anaglyph of a scene (b) Depth map computed from the epipolar geometry of the proposed coffee-filter mirror design (c) Ground Truth depth of the scene

.

(a)

(b)

(c)

Figure 8: (a) Left-eye view (b) Right-eye view (c) Red-cyan stereo image of the Patio scene [2]

.

(a)

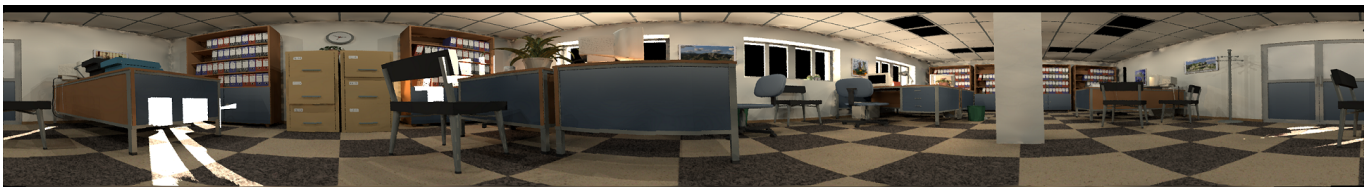

(b)

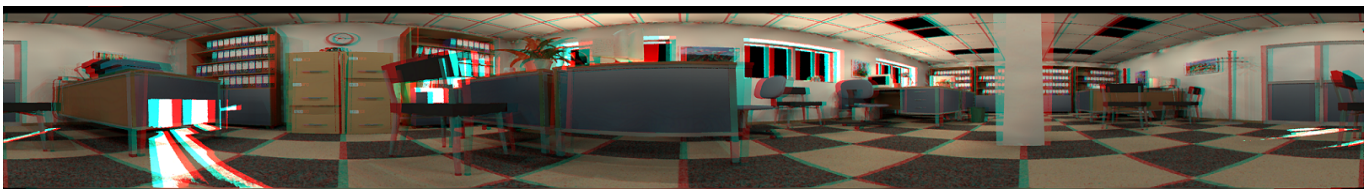

(c)

Figure 9: (a) Left-eye view (b) Right-eye view (c) Red-cyan stereo image of the Office scene [2]

.